ARTICLES

Fragmentation of Vibrationally Selected N_2O^+ in State $\tilde{C}\ ^2\Sigma^+$ from Measurements of Threshold Photoelectron Photoion Coincidence

Su-Yu Chiang* and Chien-I Ma

Synchrotron Radiation Research Center, No. 1, R&D Road VI, Hsinchu Science-Based Industrial Park, Hsinchu 300, Taiwan, Republic of China

Received: September 30, 1999; In Final Form: January 4, 2000

Dissociation of vibrationally selected N_2O^+ in state $\tilde{C}\ ^2\Sigma^+$ has been investigated with a threshold photoelectron−photoion coincidence technique in pulsed mode and with synchrotron radiation. Branching ratios and average releases of kinetic energy in channels of formation of fragments N^+, O^+, N_2^+, and NO^+ at a level below the threshold of state $\tilde{C}\ ^2\Sigma^+$, and in levels (0,0,0), (1,0,0), and (0,0,1) of that state, were obtained from well-resolved time-of-flight peaks, fitted to Gaussian shape, in the coincidence mass spectra. The results show a vibrational energy dependence, in particular, competition between channels $N^+ + NO$ and $N_2^+ + O$. On the basis of the opposite trends of branching ratios and average releases of kinetic energy of these two channels at levels (1,0,0) and (0,0,1), the dissociation mechanism and energy partition upon dissociation are discussed.

1. Introduction

State-selected chemistry providing information about branching ratios, partitions of kinetic energy released and internal energies, dissociation, and reaction rates at a specific energy level, has gained great interest in investigation of dynamics of ion dissociation and of ion-molecular reactions in the past decades.[1−3] For state-selected studies, various techniques with a laser, discharge lamp or synchrotron radiation as light source, such as multiphoton ionization (MPI) and coincidence methods, have been developed. Threshold photoelectron photoion coincidence (TPEPICO), applicable to dissociation mechanisms of a molecular ion prepared in a well-defined energy state, has been proved to be a powerful tool.[4,5] Because a continuously tunable light source is used to excite molecules to a specific energy level, this technique makes possible investigation of dissociative dynamics of molecules through both direct ionization and autoionization.

N_2O is a suitable compound for investigation of dissociation dynamics of singly ionized polyatomic molecules. Experimental techniques including absorption spectra,[6] photoelectron (PE) spectra,[7,8] electron impact (EI),[9−11] fluorescence spectra,[12−14] photoionization mass spectrometry (PIMS),[15,16] PEPICO,[17] and TPEPICO[18−20] have been applied to study the dissociative properties of N_2O^+. Theoretical calculations of potential-energy surfaces of various electronic states also have been performed in relation to detailed predissociation pathways of N_2O^+.[20−22] Therefore, valuable information on electronic states, vibrational frequencies, Rydberg series converging to various electronic states, shape resonances, and dissociation dynamics of states of selected energy is available in the literature.[6−22]

The dissociation mechanisms of N_2O^+ were investigated with excitation to mainly states $\tilde{X}\ ^2\Pi$, $\tilde{A}\ ^2\Sigma^+$, $\tilde{B}\ ^2\Pi$, and $\tilde{C}\ ^2\Sigma^+$.[9−11,16−19,23−26] It is now well established that state $\tilde{A}\ ^2\Sigma^+$ decays via fluorescence and predissociation, whereas states $\tilde{B}\ ^2\Pi$ and $\tilde{C}\ ^2\Sigma^+$ are fully predissociated. With energy in the region of state $\tilde{C}\ ^2\Sigma^+$, PI,[16] TPEPICO,[18] EI,[9−11] and PEPICO[17] studies have shown that fragments N^+, O^+, NO^+, and N_2^+ are formed on dissociation of N_2O^+, but branching ratios of these fragment ions, except for the PEPICO study, were determined either only at the (0,0,0) level from steps in the PI mass spectra or at levels (0,0,0), (1,0,0), and (0,0,1)/(2,0,0) from areas of time-of-flight (TOF) peaks in the coincidence mass spectra, which are not well resolved. Average releases of kinetic energy of N_2O^+ in these four dissociation channels, except for a weak channel for formation of O^+, were correspondingly determined from widths of the same TOF features.[18]

At the Synchrotron Radiation Research Center (SRRC), we have implemented a pulsed-field TOF mass spectrometer and have measured TPEPICO spectra of vibrationally selected N_2O^+ in state $\tilde{C}\ ^2\Sigma^+$ on a 1 m Seya−Namioka beamline.[27] Synchrotron radiation with its broadly tunable photon energy is a particularly useful source of light for this work. Use of a pulsed field improves instrumental resolution of electrons and ions and efficiency of ion collection. In this experiment, we measured well-resolved TOF peaks of fragments N^+, O^+, N_2^+, and NO^+ and fitted them at various vibrational levels to obtain branching ratios and average releases of kinetic energy in these four dissociation channels. On this basis, we discuss the dissociative properties of N_2O^+ at vibrational levels of state $\tilde{C}\ ^2\Sigma^+$.

2. Experiment

The experiment was performed on the 1.5 GeV electron storage ring operated in multibunch mode at a repetition rate of 500 MHz at SRRC in Taiwan. For our measurements on the 1 m Seya−Namioka beamline, we employed a 1200 lines/mm grating covering a spectral range of ∼500−1000 Å to disperse

* Corresponding author. Tel: (886)3-578-0281 ext 7315. Fax: (886)3-578-9816. E-mail: schiang@srrc.gov.tw.

10.1021/jp9935081 CCC: $19.00
Published on Web 02/23/2000

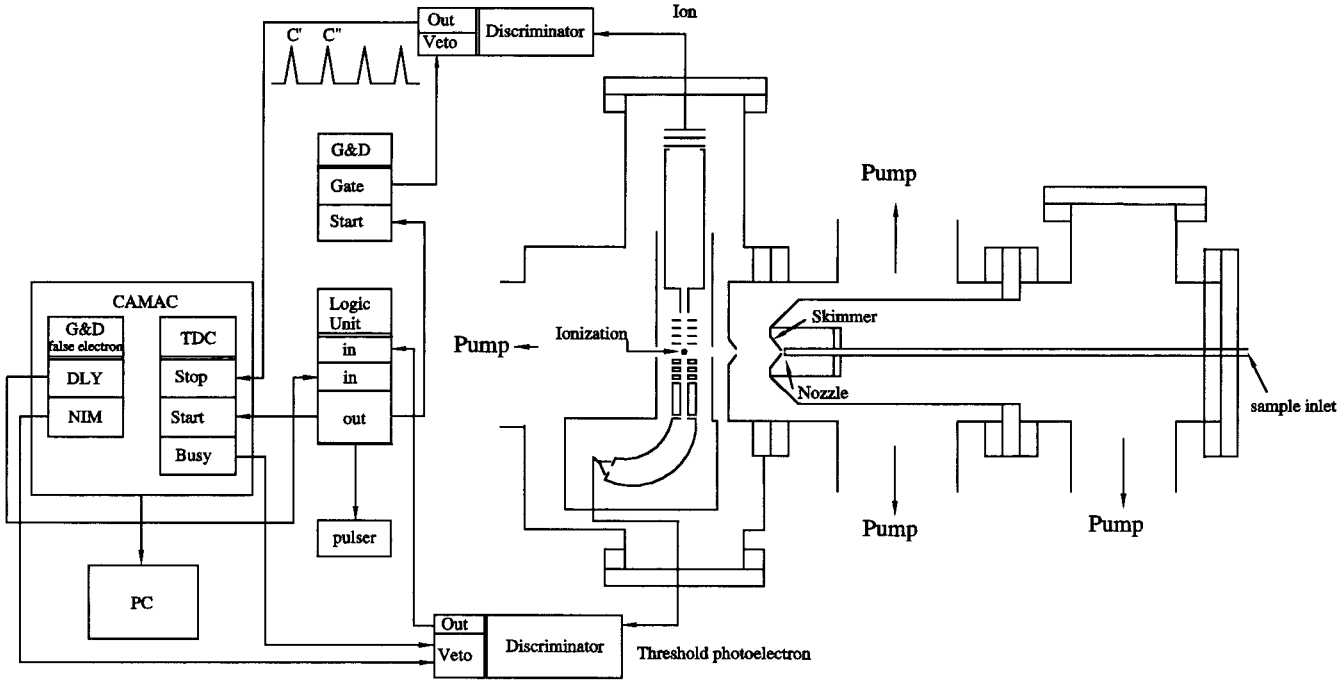

Figure 1. Schematic diagram of the molecular beam/threshold photoelectron photoion coincidence system.

the radiation. Entrance and exit slits were set at 0.05 mm to provide a wavelength resolution of ~0.5 Å in the region of 600−625 Å with photon flux > 10^9 photons/s. Photon energies were calibrated absolutely within an accuracy of 0.2 Å using known Rydberg peaks in the TPE spectrum of Ar.

Shown in Figure 1, the system for a molecular beam and threshold photoelectron photoion coincidence consists of a dual differentially pumped molecular beam source, an ionization chamber, and detectors. Sample gas at a pressure ~310−320 Torr is expanded through a nozzle of 0.125 mm diameter and skimmed with two skimmers with diameters of 1 and 2 mm to form a molecular beam. This beam is ionized by monochromatic synchrotron light crossing at a right angle in the ionization chamber. Ions and electrons produced are extracted in opposite directions toward their respective detectors, an ion TOF mass spectrometer and a threshold photoelectron spectrometer. Axes of both spectrometers are perpendicular to those of molecular and photon beams. The TOF mass spectrometer is of the Wiley−McLauren space focusing type,[28] with a drift tube of length 22 cm. The threshold photoelectron spectrometer consists of a set of 10 cm long electrostatic lenses terminated with an aperture of 2 mm diameter, followed by a 160° electrostatic energy analyzer. Dual microchannel plates serve as detectors in both spectrometers. To prevent field penetration, we covered entrance apertures of both spectrometers with gold meshes (transmission 90%). The acceleration region of the mass spectrometer and the entire electron spectrometer were also enclosed in a μ-metal shield to exclude magnetic field.

The TPE spectrum of N_2O was measured in the wavelength region of 600−625 Å, which covers the threshold of state $\tilde{C}\ ^2\Sigma^+$ and vibrational levels (0,0,0), (1,0,0), and (0,0,1). An electric field of 1.4 V/cm in the interaction region was used to extract electrons. The electron signal was fed into a counter (EG&G 9400) with output to a computer via an IEEE-488 interface. To normalize the TPE spectrum, we measured photon flux simultaneously with a Ni mesh located at the exit port of the ionization chamber.

To measure coincidence of electrons and ions, we applied a pulsed field of 48 V/cm with duration of 30 μs to extract coincident ions on detecting an electron, and an eight-channel time-to-digital converter (TDC, LeCroy 4208) to record flight times of ions for each coincidence cycle. The dead time for ion extraction is ~0.7 μs including the transit time of electrons through the threshold photoelectron spectrometer (calculated to be ~0.3 μs) and delay of electronic circuits (measured at ~0.4 μs). All data acquisition is controlled with a computer via the CAMAC interface, and output from the TDC converter is transferred to the computer for further processing.

To obtain a "true" coincidence mass spectrum, a "total" and a "false" coincidence mass spectra were accumulated; subtraction of the "false" coincidence spectrum from the "total" coincidence spectrum was then performed. The continuous nature of synchrotron radiation operating in multibunch mode results in a "total" coincidence mass spectrum triggered with electron signals having contributions from uncorrelated ions piling up in the interaction region; these uncorrelated ions constitute the "false" coincidence spectrum. To accumulate the false spectrum, we initiated a second cycle following each electron-triggered coincidence cycle with a computer-generated signal made random in time relative to the preceding electron signal. This random signal is delayed at least 100 μs from the preceding cycle to reestablish the equilibrium distribution of ions in the interaction region.

N_2O (Airgas, 99.99%) and argon (Scott Specialty Gases, 99.999%) were used without further purification.

3. Results and Discussion

3.1. Threshold Photoelectron Spectrum of State $\tilde{C}\ ^2\Sigma^+$. Figure 2 presents the TPE spectrum of N_2O^+ in state $\tilde{C}\ ^2\Sigma^+$ measured with a wavelength increment of 0.2 Å in the region of 600−625 Å. The peaks at 616.8 ± 0.2 Å (20.101 ± 0.007 eV), 612.0 ± 0.2 Å (20.258 ± 0.007 eV), and 607.9 ± 0.2 Å (20.395 ± 0.007 eV) are assigned according to the literature[7,29,30] as vibrational levels (0,0,0), (1,0,0), and (0,0,1); the three vibrational indices denote the number of quanta for symmetric stretching, bend, and asymmetric stretching modes, respectively. Level (0,0,0) at 20.101 ± 0.007 eV agrees satisfactorily with

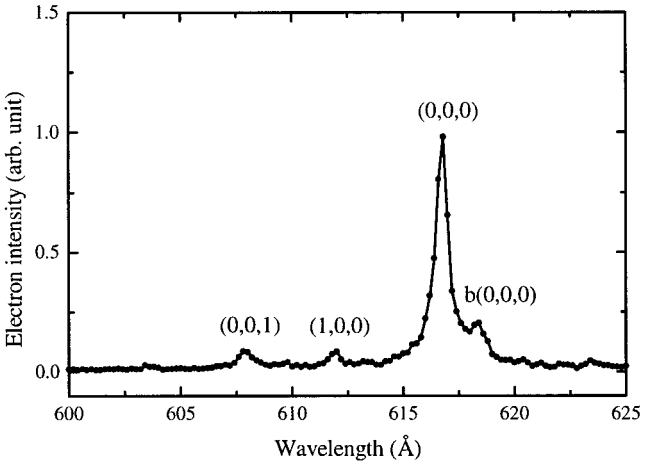

Figure 2. Threshold photoelectron spectrum of N_2O in the region 600−625 Å.

the adiabatic ionization energy of state $\tilde{C}\ ^2\Sigma^+$ measured as 20.105 eV in the PI[16] and PES[7] experiments. The vibrational intervals to levels (1,0,0) and (0,0,1) are 158 ± 7 and 294 ± 7 meV, close to the values of 150, 159, and 154 meV reported for level (1,0,0), and 295, 285, and 283 meV reported for level (0,0,1) in the literature.[7,29,30]

The peak at 618.4 Å was measured in the zero kinetic-energy photoelectron spectrum by Locht et al.[11] but not assigned. This peak is not observed in the PE spectra,[17,29] nor does it belong to a Rydberg series converging to state $\tilde{C}\ ^2\Sigma^+$ observed in the PI curves.[16] Only fragments NO^+ and N_2^+ have substantial intensities in the coincidence mass spectrum when excited to this level; this behavior is similar to that observed in dissociation of N_2O^+ in state $\tilde{B}\ ^2\Pi$. For this reason, we attribute its formation to unrevealed autoionization states converging to state $\tilde{C}\ ^2\Sigma^+$, and tentatively assign it to level b(0,0,0).

3.2. Coincidence Mass Spectra of N_2O^+. Coincidence mass spectra from dissociation of N_2O^+ in levels b(0,0,0), (0,0,0), (1,0,0), and (0,0,1) of state $\tilde{C}\ ^2\Sigma^+$ are shown in Figure 3a−d. Each spectrum, normalized to 60 000 total ion counts, shows only well-resolved and symmetrically broadened TOF distributions of fragment ions, consistent with previous reports that states $\tilde{B}\ ^2\Pi$ and $\tilde{C}\ ^2\Sigma^+$ are fully predissociated.[9−11,16−18] The TOF distribution of N_2O^+ in the coincidence spectrum excited to level (0,0,0) of state $\tilde{A}\ ^2\Sigma^+$ is narrow, with full width at half-maximum (fwhm) ∼6 ns, due to the small transverse velocity of the skimmed molecular beam in the detection axis. Hence, the broadened TOF peaks result from kinetic energy releases upon dissociation. These TOF distributions fitted to Gaussian shapes are shown as solid lines in the figures.

In Figure 3a, the substantial intensities of fragments NO^+ and N_2^+ due to excitation to level b(0,0,0) of N_2O^+ at 20.050 eV are consistent with observations in photoionization[16] and coincidence[17,19] experiments that N_2O^+ in state $\tilde{B}\ ^2\Pi$ dissociates primarily to channels $NO^+ + N$ and $N_2^+ + O$. The negligible intensity of fragment O^+ at this level also agrees with previous reports that state neither $\tilde{A}\ ^2\Sigma^+$ nor $\tilde{B}\ ^2\Pi$ yields an O^+ fragment.[17,19,20] Although in the energy range 19−20 eV, a significant production of fragments O^+ and N^+ attributed to state crossings was observed in the PEPICO study;[17] no direct comparison between PEPICO and our works can be made, due to the fact that state crossing is energy sensitive and level b(0,0,0) is unobserved or unresolved in the PE spectra, as mentioned above.[17,19,20]

As seen from Figure 3a,b, the coincidence counts of fragments N^+ and O^+ increase abruptly on excitation to level (0,0,0) of

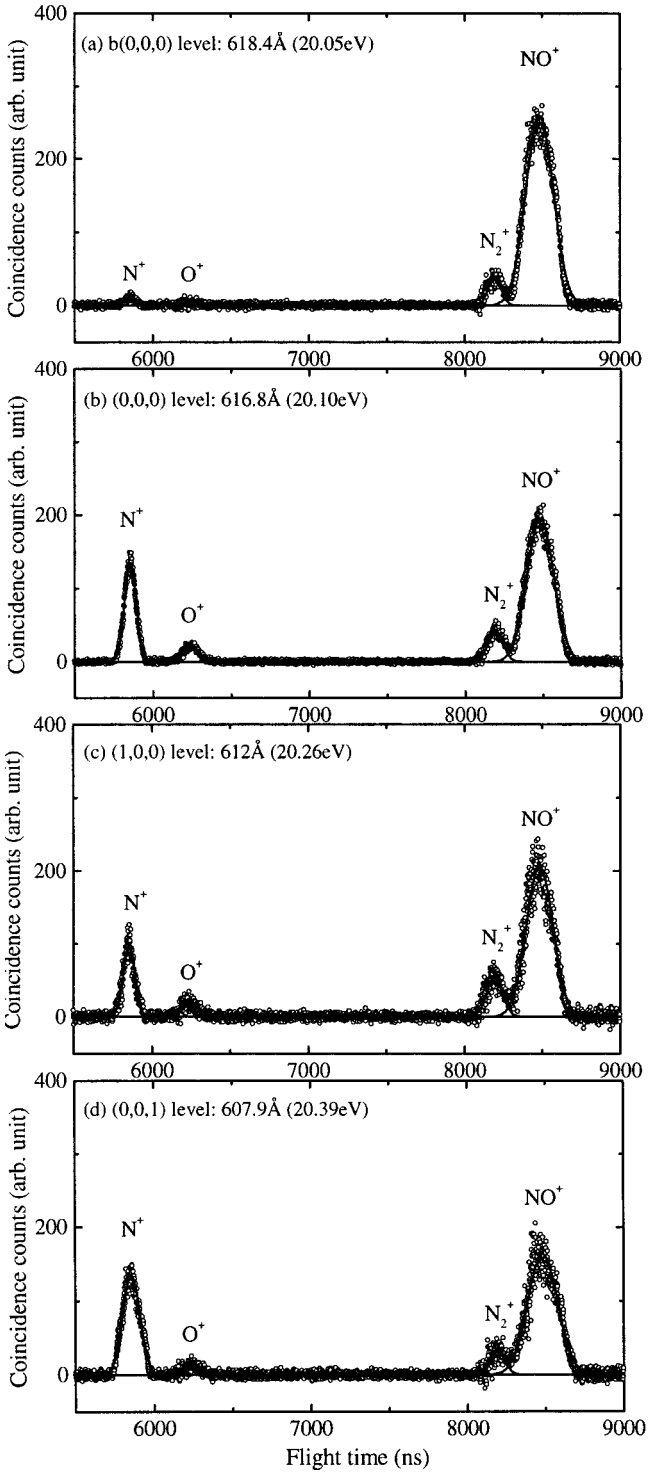

Figure 3. Coincidence spectra of N_2O excited at a level below threshold and vibrational levels (0,0,0), (1,0,0), and (0,0,1) of state $\tilde{C}\ ^2\Sigma^+$.

N_2O^+ at 20.101 eV, especially for N^+. A small increase of fragment N_2^+ and decrease of fragment NO^+ were also observed. This observation agrees with Kinmond's[17] statement that state $\tilde{C}\ ^2\Sigma^+$ is the first one to correlate directly to the formations of N^+ and O^+ and also is similar in part to "...a rather abrupt increase of fragment N^+, and proportionately smaller but distinct increases of fragment N_2^+, O^+ and NO^+ at the $\tilde{C}\ ^2\Sigma^+$ state threshold..." observed in the photoion yield curves by Berkowitz and Eland.[16] However, as dissociative properties of energy-selected ions are measured in the TPEPICO spectra, we observe more significantly increased fragment O^+

TABLE 1: Dissociation Branching Ratios of N_2O^+ with Excitation at a Level below the Threshold and Observed Vibrational Levels of State $\tilde{C}\ ^2\Sigma^+$

dissociation channel	branching ratios (%)[a]			
	b(0,0,0)	(0,0,0)	(1,0,0)	(0,0,1)
$NO^+ + N$	92 ± 2	67 ± 1	70 ± 1	63 ± 1
		57 ± 6	66 ± 6	61 ± 6[b]
		57[c]		
		74 ± 1	70 ± 1	69 ± 1[d]
$N_2^+ + O$	6 ± 2	8 ± 1	11 ± 1	6 ± 1
		24 ± 4	22 ± 4	19 ± 4[b]
		20[c]		
		10 ± 2	16 ± 3	9 ± 4[d]
$O^+ + N_2$	<1	5 ± 1	4 ± 1	2 ± 1
		1	1	3[b]
		2.2[c]		
		4 ± 2	3 ± 4	3 ± 5[d]
$N^+ + NO$	<2	20 ± 1	15 ± 1	29 ± 1
		17 ± 3	11 ± 3	17 ± 3[b]
		21[c]		
		12 ± 2	9 ± 4	18 ± 4[d]

[a] Present work, unless stated otherwise. [b] Reference 19. [c] Reference 16. [d] Reference 17.

arising from the threshold of state $\tilde{C}\ ^2\Sigma^+$ than that reported in the PI study.[16]

With N_2O^+ excited at levels b(0,0,0) and (0,0,0), formation of $NO^+(^1\Sigma^+) + N(^2P_u)$, $N_2^+(^2\Pi_u) + O(^3P_g)$, $N_2^+(^2\Sigma_g^+) + O(^1D_g)$, and $N^+(^3P_g) + NO(^2\Pi)$, are allowed both energetically and by symmetry, with their thermochemical thresholds at 17.76, 18.37, 19.22, and 19.46 eV, respectively, whereas the first symmetry-allowed channel for production of O^+ is $O^+(^2P_u) + N_2(^1\Sigma_g^+)$ at 20.31 eV.[19] Increased intensities of fragments N^+, O^+, and N_2^+ in Figure 3b indicate that a predissociative state crosses state $\tilde{C}\ ^2\Sigma^+$ at the threshold, leading to their formations. According to the theoretical calculations by Lorquet and Cadet, a predissociative state $^2\Pi$ that intersects states $\tilde{B}\ ^2\Pi$ and $\tilde{C}\ ^2\Sigma^+$ yields $O^+(^2D) + N_2(^1\Sigma_g^+)$, $N_2^+(^2\Sigma_g^+) + O(^1D_g)$, and $N^+(^3P_g) + NO(^2\Pi)$.[26] Olivier et al. proposed that a state $^2\Pi$ is responsible for formation of these three fragments in the region of state $\tilde{C}\ ^2\Sigma^+$ in their work on dissociation of N_2O by electroionization using ion kinetic energy and mass analysis.[9,10] We thus surmise that state $^2\Pi$ is related to formations of fragments observed in Figure 3b; moreover, the crossing of this state is limited to the energy region of 20.050−20.101 eV.

From Figure 3b−d excited at levels (0,0,0), (1,0,0), and (0,0,1), changes of relative intensities and bandwidths of fragment ions with vibrational levels were discerned. We discuss this behavior with variation of branching ratios.

3.3. Branching Ratios and Average Releases of Kinetic Energy. In Table 1, branching ratios of the four dissociation channels at three vibrational levels of state $\tilde{C}\ ^2\Sigma^+$ and level b(0,0,0) were obtained from the area ratios of TOF features in the coincidence mass spectra; literature values are also listed for comparison. Our results for the two major channels, $N^+ + NO$ and $NO^+ + N$, agree, within the error limits, with those reported in the PI[16] and TPEPICO[19] experiments, but not for the channels $N_2^+ + O$ and $O^+ + N_2$; our values of the channel $N_2^+ + O$ are much smaller than the literature values.[19] This discrepancy could be attributed to poorly resolved TOF features of adjacent masses, i.e., (N_2^+, NO^+) and (N^+, O^+), reported in the literature. On the other hand, our results agree satisfactorily with those obtained from well-resolved TOF features in the PEPICO[17] mass spectra, except for the channels $NO^+ + N$ and $N^+ + NO$ at levels (0,0,0) and (1,0,0). Our values of the former channel are larger but of the latter channel are much smaller than the values reported in the PEPICO study. One possible cause for this discrepancy is the different photoelectron resolution, which defines the detected ion energy range, and it is 0.05 eV in the PEPICO study and 0.025 eV in our experiment. As seen in Table 1, branching ratios change dramatically from level b(0,0,0) to level (0,0,0), even though the energy difference between these two levels is only 0.05 eV; moreover, the NO^+ fraction will increase at level (0,0,0) in low photoelectron resolution experiment due to the contribution from level b(0,0,0).

TABLE 2: Average Kinetic Energy Released in Four Dissociation Channels of N_2O^+ with Excitation at a Level below the Threshold and Observed Vibrational Levels of State $\tilde{C}\ ^2\Sigma^+$

dissociation channel	kinetic energy releases (eV)[a]			
	b(0,0,0)	(0,0,0)	(1,0,0)	(0,0,1)
$NO^+ + N$	1.44 ± 0.03	1.47 ± 0.03	1.41 ± 0.03	1.79 ± 0.03
		1.5 ± 0.3	1.6 ± 0.3	1.9 ± 0.3[b]
$N_2^+ + O$	0.33 ± 0.02	0.41 ± 0.02	0.49 ± 0.02	0.39 ± 0.02
		0.7 ± 0.15	0.6 ± 0.15	0.8 ± 0.2[b]
$O^+ + N_2$	...	0.46 ± 0.03	0.58 ± 0.03	0.46 ± 0.03
$N^+ + NO$	0.22 ± 0.02	0.28 ± 0.02	0.27 ± 0.02	0.6 ± 0.03
		0.6 ± 0.15	0.6 ± 0.15	0.6 ± 0.15[b]

[a] Present work, unless stated otherwise. [b] Reference 19.

Table 2 lists the calculated average kinetic energies released in the channels $NO^+ + N$, $N_2^+ + O$, $N^+ + NO$, and $O^+ + N_2$ when N_2O^+ is excited to the four levels. As shown in Figure 3, the broadened TOF feature of each fragment ion is fitted with a Gaussian shape. In general, for a TOF distribution of this type, the average release of kinetic energy is related to the fwhm of the TOF feature; for this reason we calculate the average release of kinetic energy of each dissociation channel according to the following equation.[31,32]

$$\langle \mathrm{KER} \rangle = \frac{3}{15 \ln 2} \epsilon^2 (\mathrm{fwhm})^2 \frac{M_p}{M_f (M_p - M_f)} - \frac{3}{2} RT \frac{M_f}{(M_p - M_f)} \quad (1)$$

in which $\langle KER \rangle$ is the average release of kinetic energy of a specific dissociation channel, $\epsilon = 35$ V/cm is the strength of the electric field, M_p and M_f are masses of parent and fragment ions, and $T = 2$ K is the transverse temperature of the molecular beam, calculated from fwhm 6 ns of the parent ion TOF feature.

Literature values of all channels but $O^+ + N_2$ excited to levels (0,0,0), (1,0,0), and (0,0,1) are listed in Table 2 for comparison. Our values for the channel $NO^+ + N$ for N_2O^+ excited to all levels and for the channel $N^+ + NO$ for N_2O^+ excited to level (0,0,1) agree satisfactorily with those reported in the literature.[19] Significant differences are also observed, i.e., more than 50% for the channel $N^+ + NO$ for N_2O^+ excited to levels (0,0,0) and (1,0,0), and ~20−50% for the channel $N_2^+ + O$ for N_2O^+ excited to all levels. For the channel $N^+ + NO$, kinetic energy release was reported to peak at 0.25 eV and with a maximum at ~0.4 eV in the PEPICO experiment;[17] this result agrees with our average release of kinetic energy 0.28 eV. We thus attribute the discrepancy to poorly resolved TOF features of adjacent masses reported in the literature, as mentioned above.[19]

3.4. Dissociative Properties. The branching ratios listed in Table 1 show dependence on vibrational energy of the parent ion. The values for channels $NO^+ + N$ and $N_2^+ + O$ increase from level (0,0,0) to (1,0,0) but decrease from the latter level to (0,0,1), whereas channel $N^+ + NO$ displays an opposite trend. Nenner et al.[19] observed a similar phenomenon for fragment N^+, and Kinmond et al.[17] found a competition between fragments N^+ and N_2^+, but no explanation was given in both

TABLE 3: Internal Energy of Fragments at Various Vibrational Levels of State $\tilde{C}\ ^2\Sigma^+$ Calculated from Dissociation Thresholds and Measured Kinetic Energy Releases

fragments and states	dissociation threshold/eV	E_{int}/eV at (0,0,0)	at (1,0,0)	at (0,0,1)
$NO^+ + N$				
$^1\Sigma^+ + {}^2P$	17.76	0.87	1.09	0.84
$N_2^+ + O$				
$^2\Sigma_g^+ + {}^1D$	19.22	0.47	0.55	0.78
$N_2 + O^+$				
$^1\Sigma_g^+ + {}^2D$	18.61	1.03	1.07	1.32
$NO + N^+$				
$^2\Pi + {}^3P$	19.46	0.36	0.53	0.33

cases. We discuss this behavior in more detail, but for channel $O^+ + N_2$, we ignore its role because of the small contribution.

The variation in branching ratios is easily recognized on comparing the fraction of variation of each channel at various vibrational levels. From level (0,0,0) to (1,0,0), the ratios of channels $NO^+ + N$ and $N_2^+ + O$ increase ~4% and ~40%, respectively, whereas that of channel $N^+ + NO$ decreases ~25%. In contrast, a decrease of ~10% and ~50% of the former two channels and an increase of >90% of the latter channel are observed from level (1,0,0) to (0,0,1). The variation of dominant channel $NO^+ + N$ is obviously much less than those of the other two channels; channel $N_2^+ + O$ becomes more competitive than channel $N^+ + NO$ at level (1,0,0), whereas the situation is reversed at level (0,0,1).

Like the branching ratios, the fwhm of fragments N^+ and N_2^+ follow opposite trends across the three vibrational levels, as shown in Figure 3b−d. Trends reflected in average release of kinetic energy are correspondingly observed in Table 2, in which the values for channel $N_2^+ + O$ are 0.33, 0.41, 0.49, and 0.39 eV from level b(0,0,0) to (0,0,1); in contrast, the values for channel $N^+ + NO$ are 0.22, 0.28, 0.27, and 0.6 eV. Obviously, these results show that excess vibrational energy of the parent ion is converted to internal energy of fragments preferentially at specific levels during dissociation, specifically, vibrational energies of fragment NO in the channel $N^+ + NO$ at the (1,0,0) level and fragment N_2^+ in the channel $N_2^+ + O$ at level (0,0,1).

Table 3 lists average internal energies for each dissociation channel calculated from dissociation thresholds adopted from the literature[19] and our derived average kinetic energies. As expected, the internal energy 0.53 eV of fragment NO at level (1,0,0) exceeds the value of 0.33 eV at level (0,0,1) and 0.36 eV at (0,0,0) for channel $N^+ + NO$; the value of 0.78 eV at level (0,0,1) for fragment N_2^+ in channel $N_2^+ + O$ is the largest compared with the values of 0.55 eV at level (1,0,0) and 0.47 eV at (0,0,0). According to the vibrational frequency 1876 cm^{-1} and anharmonicity constant 13.97 cm^{-1} of NO,[33] vibrational energies at levels $v = 1-4$ are 0.233, 0.462, 0.688, and 0.910 eV, respectively. Our result thus shows that most NO fragments are likely populated at $v = 1$ excited at levels (0,0,0) and (0,0,1) of N_2O^+ and $v = 2$ at level (1,0,0). Similarly, for channel $N_2^+ + O$, vibrational energies of 0.270, 0.536, and 0.797 eV correspond respectively to N_2^+ $v = 1-3$ when vibrational frequency 2175 cm^{-1} and anharmonicity constant 16.14 cm^{-1} are adopted.[33] Most N_2^+ fragments are likely populated at $v = 1$ and 2 at levels (0,0,0) and (1,0,0) of N_2O^+, and $v = 2$ and 3 at level (0,0,1).

This analysis reveals a correlation between the rate of dissociation and the conversion of internal energy, which results in variation of branching ratios in these two channels: the dissociation rates become smaller as the vibrational energy of fragments increases. In addition, fragments NO are mostly populated at $v = 1$ at level (0,0,1) or at $v = 2$ at level (1,0,0) although the excitation energy 20.395 eV of level (0,0,1) exceeds that of 20.258 eV of level (1,0,0). As noted above, a state $^2\Pi$ leading to predissociation of state $\tilde{C}\ ^2\Sigma^+$ is proposed to be responsible for formation of channels $O^+ + N_2$, $N_2^+ + O$, and $N^+ + NO$.[9,10,26] Our observations can be explained in terms of an effect of vibrational energy on state crossing, which causes dissociation to be less favored along coordinate $(N-NO)^+$ at level (1,0,0), and less favored along coordinate $(N_2-O)^+$ at level (0,0,1).

In addition to the effect of vibrational energy, the vibrational mode could also affect the branching ratios. Richard-Viard et al. have found that the vibrational distributions of fragment NO^+ depend on the nature and the number of vibrational quanta excited in the predissociation studies of the $\tilde{A}\ ^2\Sigma^+$ state.[20] However, discussion of this effect will not be addressed in this paper.

4. Conclusions

From the well-resolved TOF features of fragments N^+, O^+, N_2^+, and NO^+ in the coincidence mass spectra, we attribute the distinct increases of fragments N^+, O^+, and N_2^+ at the threshold of state $\tilde{C}\ ^2\Sigma^+$ to predissociation of state $\tilde{C}\ ^2\Sigma^+$ by crossing with a state $^2\Pi$. We derived branching ratios and average releases of kinetic energy for the channels $NO^+ + N$, $N_2^+ + O$, $O^+ + N_2$, and $N^+ + NO$. The branching ratios and the average release of kinetic energy depend on vibrational energy in the precursor ion, especially for channels $N_2^+ + O$ and $N^+ + NO$, for which a competition exists at levels (1,0,0) and (0,0,1) of N_2O^+. This competition is attributed to increased conversion of excess energy of parent ions into vibrational energy of NO fragments at level (1,0,0) and of N_2^+ fragments at level (0,0,1), which results in slow dissociation. The average internal energies of all dissociation channels at several vibrational levels are derived from the measured kinetic energies and dissociation thresholds, which provide estimates of vibrational populations of fragments NO and N_2^+.

Acknowledgment. One of the authors (S.-Y.) is grateful to Professor T. Baer for reading their manuscript. We thank the Synchrotron Radiation Research Center and the National Science Council of Taiwan for financial support of this work (Contract No. NSC88-2613-M-213-019-L1).

References and Notes

(1) Baer, T. *Adv. Chem. Phys.* **1986**, *64*, 111.
(2) Farrar, J. M.; Saunders: W. H. *Technique for the Study of Ion−Molecule Reactions*; Wiley: New York USA, 1988; Vol. XX.
(3) Jennings, K. R. *Fundamentals of Gas-Phase Ion Chemistry*; Kluwer: Dordrecht, Netherlands, 1991.
(4) Guyon, P. M.; Baer, T.; Ferreira, L. F. A.; Nenner, I.; Tabché-Fouhailé, A.; Botter, R.; Govers, T. R. *J. Phys. B* **1978**, *11*, L141.
(5) Marr, G. V. *Handbook on Synchrotron Radiation*; Amsterdam: North-Holland, 1987; Vol. 2.
(6) Tanaka, Y.; Jursa, A. S.; LeBlanc, F. J. *J. Chem. Phys.* **1960**, *32*, 1205.
(7) Dehmer, P. M.; Dehmer, J. L.; Chupka, W. A. *J. Chem. Phys.* **1980**, *73*, 126.
(8) Cvitaš, T.; Klasinc, L.; Kovac, B.; McDiarmid, R. *J. Chem. Phys.* **1983**, *79*, 1565.
(9) Olivier, J. L.; Locht, R.; Momingy, J. *Chem. Phys.* **1984**, *84*, 295.
(10) Olivier, J. L.; Locht, R.; Momingy, J. *Chem. Phys.* **1982**, *68*, 201.
(11) Locht, R.; Hagenow, G.; Hottmann, K.; Baumgärtel, H. *Chem. Phys.* **1991**, *151*, 137.
(12) Frey, R.; Gotchev, B.; Peatman, W. B.; Pollak, H.; Schlag, E. W. *Chem. Phys. Lett.* **1978**, *54*, 411.
(13) Kelly, L. A.; Duffy, L. M.; Space, B.; Poliakoff, E. D.; Roy, P.; Southworth, S. H.; White, M. G. *J. Chem. Phys.* **1989**, *90*, 1544.

(14) Tokue, I.; Kobayashi, M.; Ito, Y. *J. Chem. Phys.* **1992**, *96*, 7458.
(15) Coppens, P.; Smets, J.; Fishel, M. G.; Drowart, J. *Int. J. Mass Spectrom. Ion Phys.* **1974**, *14*, 57.
(16) Berkowitz, J.; Eland, J. H. D. *J. Chem. Phys.* **1977**, *67*, 2740.
(17) Kinmond, E.; Eland, J. H. D.; Kaslsson, L. *Int. J. Mass Spectrom.* **1999**, *185*−*187*, 437.
(18) Eland, J. H. D. *Int. J. Mass Spectrom. Ion Phys.* **1973**, *12*, 389.
(19) Nenner, I.; Guyon, P. M.; Baer, T.; Govers, T. R. *J. Chem. Phys.* **1980**, *72*, 6587.
(20) Richard-Viard, M.; Atabek, O.; Dutuit, O.; Guyon, P. M. *J. Chem. Phys.* **1990**, *93*, 8881.
(21) Hopper, D. G. *Chem. Phys. Lett.* **1975**, *31*, 446.
(22) Hopper, D. G. *J. Am. Chem. Soc.* **1978**, *100*, 1019.
(23) Lermé, J.; Abed, S.; Larzillière, M.; Holt, R. A.; Carré, M. *J. Chem. Phys.* **1986**, *84*, 2167.
(24) Brehm, B.; Frey, R.; Küstler, A.; Eland, J. H. D. *Int. J. Mass Spectrom. Ion Phys.* **1974**, *13*, 251.
(25) Masuoka, T.; Mitani, S. *J. Chem. Phys.* **1989**, *90*, 2651.
(26) Lorquet, I. C.; Cadet, C. *Int. J. Mass Spectrom. Ion Phys.* **1971**, *7*, 254.
(27) Tseng, P.-C.; Hsieh, T.-F.; Song, Y.-F.; Lee, K.-D.; Chung, S.-C.; Chen, C.-I.; Lin, H.-F.; Dann, T. E.; Huang, L.-R.; Chen, C.-C.; Chuang, J. M.; Tsang, K.-L.; Chang, C.-N. *Rev. Sci. Instrum.* **1995**, *66*, 1815.
(28) Wiley, W. C.; McLaren, I. H. *Rev. Sci. Instrum.* **1955**, *26*, 1150.
(29) Weiss, M. J. *Chem. Phys. Lett.* **1976**, *39*, 250.
(30) Brundle, C. R.; Turner, D. W. *Int. J. Mass Spectrom. Ion Phys.* **1969**, *2*, 195.
(31) Stockbauer, R. *Int. J. Mass Spectrom. Ion Phys.* **1977**, *25*, 89.
(32) Baer, T.; Whillett, G. D.; Smith, D.; Phillips, J. S. *J. Chem. Phys.* **1979**, *70*, 4076.
(33) Herzberg, G. *Molecular Spectra and Molecular Structure, Vol. I: Spectra of Diatomic Molecules*, Reprint Edition; Krieger Publishing Co.: Florida, 1989.